Proc. Natl. Acad. Sci. USA
Vol. 96, pp. 10164–10169, August 1999
Cell Biology

Syntaxin 1 interacts with the L_D subtype of voltage-gated Ca^{2+} channels in pancreatic β cells

SHAO-NIAN YANG*, OLOF LARSSON*†, ROBERT BRÄNSTRÖM*, ALEJANDRO M. BERTORELLO*, BARBARA LEIBIGER*, INGO B. LEIBIGER*, TILO MOEDE*, MARTIN KÖHLER*, BJÖRN MEISTER‡, AND PER-OLOF BERGGREN*

*The Rolf Luft Center for Diabetes Research, Department of Molecular Medicine, and ‡Department of Neuroscience, Karolinska Institutet, Karolinska Hospital, S-171 76 Stockholm, Sweden

Communicated by Rolf Luft, Karolinska Hospital, Stockholm, Sweden, June 28, 1999 (received for review April 7, 1999)

ABSTRACT **Interaction of syntaxin 1 with the α_{1D} subunit of the voltage-gated L type Ca^{2+} channel was investigated in the pancreatic β cell. Coexpression of the enhanced green fluorescent protein-linked α_{1D} subunit with the enhanced blue fluorescent protein-linked syntaxin 1 and Western blot analysis together with subcellular fractionation demonstrated that the α_{1D} subunit and syntaxin 1 were colocalized in the plasma membrane. Furthermore, the α_{1D} subunit was coimmunoprecipitated efficiently by a polyclonal antibody against syntaxin 1. Syntaxin 1 also played a central role in the modulation of L type Ca^{2+} channel activity because there was a faster Ca^{2+} current run-down in cells incubated with antisyntaxin 1 compared with controls. In parallel, antisyntaxin 1 markedly reduced insulin release in both intact and permeabilized cells, subsequent to depolarization with K^+ or exposure to high Ca^{2+}. Exchanging Ca^{2+} for Ba^{2+} abolished the effect of antisyntaxin 1 on both Ca^{2+} channel activity and insulin exocytosis. Moreover, antisyntaxin 1 had no significant effects on Ca^{2+}-independent insulin release trigged by hypertonic stimulation. This suggests that there is a structure–function relationship between the α_{1D} subunit of the L type Ca^{2+} channel and the exocytotic machinery in the pancreatic β cell.**

Syntaxin 1 plays a central role in exocytosis from pancreatic β cells (1–3). Thus, it has been demonstrated that exposure of permeabilized mouse pancreatic β cells to antibodies against syntaxin 1 significantly inhibits Ca^{2+}-induced insulin secretion (1). Furthermore, synthetic peptides, corresponding to the H3 region of the carboxyl-terminal domain of syntaxin 1, markedly inhibit Ca^{2+}-dependent insulin secretion from permeabilized pancreatic β cells (2).

In neurons, syntaxin interacts not only with other synaptic proteins but also with voltage-dependent Ca^{2+} channels (4, 5). Several studies indicate that the interaction between syntaxin and voltage-dependent Ca^{2+} channels results in a functional modulation of the Ca^{2+} current. Thus, electrophysiological studies have shown that syntaxin modulates N, L_C, and Q type Ca^{2+} currents in *Xenopus* oocytes, coexpressing voltage-gated Ca^{2+} channels and syntaxin (6–8). It also has been reported that intracellular application of a synthetic peptide fragment of the α_{1C} subunit diminished exocytosis from the pancreatic β cell via interference with the interaction of the L type Ca^{2+} channel with the exocytotic machinery. However, analysis of mRNAs encoding the α_{1C} and α_{1D} subunits implies that the Ca^{2+}-conducting subunits of the L type Ca^{2+} channel in the pancreatic β cell mainly consist of the α_{1D} subunit (9, 10).

We now show that syntaxin 1 colocalizes and associates with the α_{1D} subunit of the voltage-gated L type Ca^{2+} channel and thereby modulates not only Ca^{2+} channel activity but also insulin release in a Ca^{2+}-dependent manner.

MATERIALS AND METHODS

Preparation of Islets and Single β cells. Islets of Langerhans and single pancreatic β cells were isolated from adult obese mice (gene symbol ob/ob) as described previously (11).

Coexpression of α_{1D} Subunit–Enhanced Green Fluorescent Protein (EGFP) and Enhanced Blue Fluorescent Protein (EBFP)–Syntaxin 1 and Fluorescence Microscopy. The cDNA for hamster α_{1D3a} (provided by J. Dillon, New England Medical Center, Boston) was flanked with the human cytomegalovirus (CMV) promoter and the bovine growth hormone poly(A) site to enable expression in mammalian cells. A *Hin*dIII site was introduced by site-directed mutagenesis at the nucleotides coding for the last amino acid and the stop codon, which allowed in-frame fusion with the EGFP cDNA and generation of pCMV α_{1D3a} EGFP. To create pCMV EBFP-syntaxin 1A, a *Sma*I site was introduced into the EBFP cDNA at the nucleotides coding for Asp-235 and Glu-237, generating pCMV EBFP0. The cDNA for rat syntaxin 1A (gift from R. H. Scheller, Stanford University, Stanford, CA) was removed from pRcCMV syntaxin 1A by digestion with *Eco*RV and *Xba*I and fused in-frame with the EBFP cDNA of the *Sma*I/*Xba*I-opened pCMV EBFP0. Cultured single pancreatic β cells were cotransfected with pCMV α_{1D3a} EGFP and pCMV EBFP-syntaxin 1A overnight by the lipofectamine technique. The cotransfected cells were monitored for EGFP/EBFP fluorescence 48 h after the start of transfection by using a Leica Fluovert FU microscope (Leica, Deerfield, IL) and PL Fluotar 100/1.32 oil lens (Leitz) equipped with a LSR AstroCam TE3/A/S charge-coupled device camera (LSR, Cambridge, U.K.). Filter settings for EGFP fluorescence measurements were: excitation, HQ470/40; dichroic mirror, Q495LP; and emission, HQ525/50. Filter settings for EBFP fluorescence measurements were: excitation, D399/22; dichroic mirror, 420DLCP; and emission, E430LP. Colocalization of α_{1D3a} EGFP and EBFP-syntaxin 1A was studied by applying the deconvolution method on a stack of 15 images (200-nm vertical distance) using the iterative Tikhonov–Miller restoration procedure (Huygens System 2; Scientific Volume Imaging, Hilversum, The Netherlands).

Density Gradient Subcellular Fractionation. Subcellular fractionation, using a linear sucrose gradient, was performed as described previously (12).

Gel Electrophoresis and Western Blot Analysis. Proteins (90 μg/slot) from individual fractions were separated in discontinuous gels consisting of a stacking gel (3% acrylamide) and a separating gel, SDS-polyacrylamide gradient gel (6.6–13.3% acrylamide). The separated proteins then were electroblotted to hydrophobic polyvinylidene difluoride membrane (Hybond-P). The blots were blocked by incubation for 2 h with

The publication costs of this article were defrayed in part by page charge payment. This article must therefore be hereby marked "*advertisement*" in accordance with 18 U.S.C. §1734 solely to indicate this fact.

PNAS is available online at www.pnas.org.

Abbreviations: EBFP, enhanced blue fluorescent protein; EGFP, enhanced green fluorescent protein; GST, glutathione *S*-transferase; CMV, cytomegalovirus; 5-HTP, 5-hydroxy-DL-tryptophan.

†To whom reprint requests should be addressed at: Karolinska Hospital (L1:02), S-171 76 Stockholm, Sweden. E-mail: olof@enk.ks.se.

7.5% nonfat milk powder in tris(hydroxymethyl)aminomethane-buffered saline and then incubated overnight at 4°C with polyclonal anti-α_{1D} subunit (1:200; Alomone Labs, Jerusalem), anti-NKα1 (1:1,000; courtesy of M. Caplan, Yale University, New Haven, CT), and monoclonal antisyntaxin (clone HPC-1, 1:500; Sigma), respectively. After washing with tris(hydroxymethyl)aminomethane-buffered saline, the blots were incubated with the secondary antibodies [horseradish peroxidase-conjugated goat anti-mouse IgG or horseradish peroxidase-conjugated goat anti-rabbit IgG; 1:50,000 in tris(hydroxymethyl)aminomethane-buffered saline; Bio-Rad] at room temperature for 1 h. The immunoreactive bands were visualized with ECL Plus Western blotting detection system (Amersham Pharmacia).

Immunoprecipitation. The pooled plasma membrane fractions (from no. 4 to no. 9) from mouse pancreatic islets of Langerhans were solubilized in 1% CHAPS after 2 h of incubation in the buffer containing 1 mM $CaCl_2$, 170 mM tris(hydroxymethyl)aminomethane-HCl, pH 7.4. The CHAPS extract was subjected to immunoprecipitation with polyclonal antisyntaxin 1 (Alomone Labs), nonimmune rabbit IgG, and protein A-Sepharose (Amersham Pharmacia) or with monoclonal antisyntaxin 1 (Sigma) and nonimmune mouse IgG precoupled to protein G-Sepharose (Amersham Pharmacia). To investigate possible binding of syntaxin 1 to polyclonal antisyntaxin 1, monoclonal antisyntaxin 1, or nonimmune IgG coupled to protein A- or G-Sepharose and of α_{1D} subunit to syntaxin 1, SDS/PAGE and Western blot analyses were performed.

Patch-Clamp and Amperometry Recordings. Whole-cell Ca^{2+} currents were recorded as described previously (13) in pancreatic β cells incubated with monoclonal antisyntaxin 1 (1:200; Sigma), monoclonal antitubulin (1:200; Sigma), normal extracellular solution, or monoclonal antisyntaxin 1 (1:200) preabsorbed with glutathione *S*-transferase (GST)–syntaxin 1A (240 μg/ml diluted antibody), respectively, for 1 h.

Amperometry recordings were performed as described previously (13). Six to 12 h before the experiment, cells were preincubated in 5-hydroxy-DL-tryptophan (5-HTP; Sigma). 5-HTP was prepared as stock solutions with a concentration of 25 mM and then added to the culture medium at a final concentration of 1 mM. 5-HTP is converted to serotonin in the β cell, and it is well established that serotonin is loaded primarily into secretory vesicles, being cosecreted with insulin by exocytosis (14). Cells were stimulated by a transient (30-s) pulse of extracellular solution, with the K^+ concentration elevated to 50 mM or with 500 mOsM sucrose by using a flow-injector (Transjector, Eppendorf, Germany).

Cell Permeabilization and Radioimmunoassay. Cells were electropermeabilized as described previously (15). After permeabilization, the cell suspension was spun down, resuspended, and incubated with intracellular buffer with or without monoclonal antisyntaxin (1:200) or mouse IgG (1:200) in the absence of both Ca^{2+} and Ba^{2+} or in the presence of 10 μM Ca^{2+} and/or 100 μM Ba^{2+} at 37°C for 10 min. Insulin release was measured by standard radioimmunoassay (15).

RESULTS

Localization of the α_{1D} Subunit and Syntaxin 1 in Pancreatic β Cells. Coexpression of the EGFP-linked α_{1D} subunit and EBFP-linked syntaxin 1 together with the deconvolution of fluorescence images showed the profiles of α_{1D} subunit-EGFP and EBFP-syntaxin 1 in the same β cell (Fig. 1*A*). Green (Fig. 1*A Left*) and red (Fig. 1*A Center*) represent the digital pseudocolor for the fluorescence emitted from EGFP and EBFP, respectively. The two fluorescence signals were observed mainly in the plasma membrane region of the cell. The yellow color (Fig. 1*A Right*) obtained by overlaying the EGFP signal with the EBFP signal indicated colocalization of the expressed α_{1D} subunit-EGFP with EBFP-syntaxin 1 in the plasma membrane.

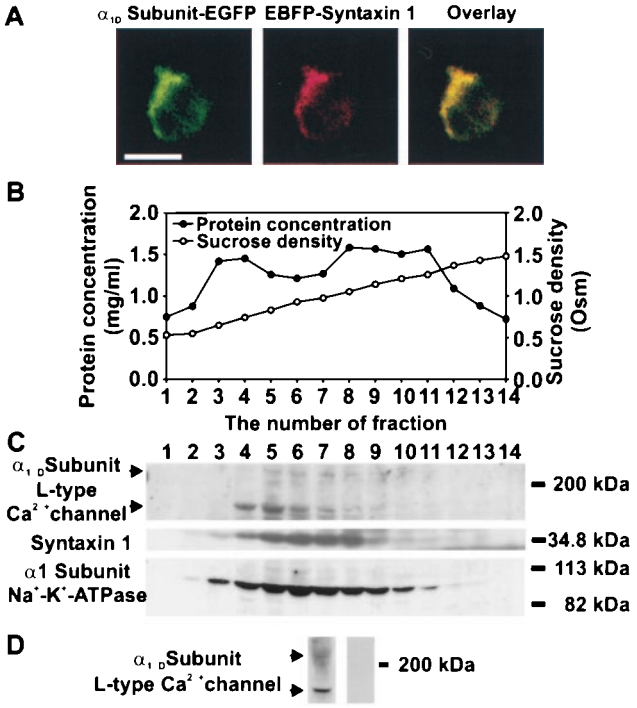

FIG. 1. Localization of the α_{1D} subunits of the L type Ca^{2+} channel and syntaxin 1 in the pancreatic β cell. (*A*) Fluorescence images of the coexpressed α_{1D} subunit-EGFP with EBFP-syntaxin 1 in the same pancreatic β cell. The cotransfected cells were monitored for EGFP/EBFP fluorescence 48 h after the start of transfection. The green color is used as the digital pseudocolor for the fluorescence emitted from EGFP (*Left*) and the red is used as the digital pseudocolor for the fluorescence emitted from EBFP (*Center*). The yellow color (*Right*), obtained after overlaying the deconvoluted EGFP and EBFP signals, indicated the colocalization of the expressed α_{1D}-EGFP with EBFP-syntaxin 1 in the plasma membrane. (Bar = 10 μm.) (*B*) Distribution of protein and sucrose density in 14 fractions collected from a linear sucrose density gradient (0.53–1.48 M). The postnuclear supernatants were loaded onto a linear sucrose density gradient, centrifuged at 120,000 × *g*, and fractions were collected. The sucrose density was measured by refractometry. (*C*) Subcellular distribution of the two isoforms (upper arrow, 210 kDa; lower arrow, 180 kDa) of the α_{1D} subunit, syntaxin 1, and Na^+-K^+-ATPase α1 subunit in 14 fractions from mouse pancreatic islets. The immunoreactive bands were visualized with ECL Plus Western blotting detection system. The experiments were repeated three times. (*D*) Specific immunoreactivity of the α_{1D} subunit of the L type Ca^{2+} channel in the plasma membrane fraction (no. 6) from mouse islets. Polyclonal antibody against the α_{1D} subunit recognized two major bands of proteins (*Left*) with molecular masses of 210 (upper arrow) and 180 kDa (lower arrow). Specific interaction of the antibody with the α_{1D} subunit was inhibited fully by preabsorption (*Right*) with the antigen peptide CND1.

To confirm further the colocalization of the α_{1D} subunit and syntaxin 1 in the plasma membrane and to characterize the membrane fractions to be used in immunoprecipitation experiments, the subcellular distribution pattern, using a linear sucrose gradient (Fig. 1*B*), of the α_{1D} subunit and syntaxin 1 was visualized by Western blot analysis. The antibody against the α_{1D} subunit recognized two bands of proteins with molecular masses of 210 and 180 kDa (Fig. 1*C Top*), respectively, concentrated mainly in fractions 4–8. The distribution of immunoreactivity for syntaxin 1 was similar to that of the α_{1D} subunit and, thus, predominately located in fractions 4–8 (Fig. 1*C Middle*) corresponding to the plasma membrane. The Na^+-K^+-ATPase α1 (Nkα1) subunit was used as a marker for the plasma membrane (Fig. 1*C Bottom*) (16).

That the antibody against the α_{1D} subunit specifically recognized two bands of proteins (Fig. 1 *C Top* and *D Left*) with molecular masses of 210 and 180 kDa, respectively, is in agreement with previous findings (17). To test further the specificity of the antibody against the α_{1D} subunit, the blot was incubated with anti-α_{1D} subunit antibodies preabsorbed with the antigen peptide, CND1. After preabsorption, no signal from the α_{1D} subunit could be detected (Fig. 1*D Right*).

Association of Syntaxin 1 with the α_{1D} Subunits in the Plasma Membrane of Pancreatic β Cells. To test for association of syntaxin 1 with the α_{1D} subunit in the plasma membrane, immunoprecipitation was performed with a polyclonal antibody against the intracellular domain of syntaxin 1 and a mAb to the extracellular domain of syntaxin 1. As shown in Fig. 2, the polyclonal antibody against the intracellular domain of syntaxin 1 not only immunoprecipitated syntaxin 1 (Fig. 2, lane 1, lower blot), but also pulled down the two isoforms [Fig. 2, upper arrow (210 kDa) and lower arrow (180 kDa)] of the α_{1D} subunit (Fig. 2, lane 1, upper blot). In contrast, the mAb to the extracellular domain of syntaxin 1 only immunoprecipitated syntaxin 1 (Fig. 2, lane 3, lower blot) without a detectable associated α_{1D} subunit (Fig. 2, lane 3, upper blot). Nonimmune rabbit or mouse IgG could not pull down either syntaxin 1 (Fig. 2, lanes 2 and 4, lower blots) or the α_{1D} subunit (Fig. 2, lanes 2 and 4, upper blots).

Effects of Antisyntaxin 1 on L type Ca^{2+} Currents in Pancreatic β Cells. Pancreatic β cells were incubated with normal extracellular solution in the absence (Fig. 3*A*) or presence (Fig. 3*C*) of the mAb against tubulin (1:200) and with the monoclonal antisyntaxin 1 (1:200) preabsorbed with GST-syntaxin 1A (Fig. 3*D*, 240 μg/ml diluted antibody), respectively. Typical L type Ca^{2+} current traces evoked by repetitive depolarizing voltage pulses from a holding potential of -70 mV to 0 mV (100 ms, 0.05 Hz) were not significantly different between the three different groups of cells, as shown by the 15 superimposed current traces. In contrast, the same voltage protocol resulted in a gradual decrease in the Ca^{2+} currents (Fig. 3*B*) after incubation with the mAb against syntaxin 1 (1:200). Compiled data, as shown in Fig. 3*E*, show that L type Ca^{2+} currents ran down significantly faster in cells incubated with antisyntaxin 1 compared with control cells or cells incubated with antitubulin.

Previous studies have shown that the H3 region (N type Ca^{2+} channel-binding domain) of syntaxin is responsible for Ca^{2+}-induced insulin release (2) and interacts with the α_{1B} subunit of the N type Ca^{2+} channel in a Ca^{2+}-dependent manner (18). To test whether the inhibitory effect of antisyntaxin 1 on the L type Ca^{2+} channel was Ca^{2+}-dependent, Ca^{2+} was replaced with equimolar concentrations of Ba^{2+} (10 mM) in the extracellular solution. As shown in Fig. 3 *F–H*, 15

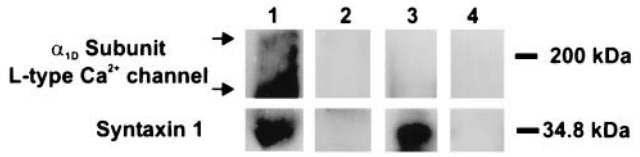

FIG. 2. Association of syntaxin 1 with the α_{1D} subunit of the voltage-gated L type Ca^{2+} channel in plasma membrane of mouse pancreatic β cells. The pooled plasma membrane fractions (four to eight) were solubilized in CHAPS and then subjected to immunoprecipitation with polyclonal antisyntaxin 1 (lane 1), nonimmune rabbit IgG (lane 2), monoclonal antisyntaxin 1 (lane 3), and nonimmune mouse IgG (lane 4). Syntaxin 1 (lower blots) and the α_{1D} subunit (upper blots) were visualized by SDS/PAGE and Western blotting and the ECL Plus detection system. Syntaxin 1 bound to both the polyclonal antisyntaxin 1 (lane 1) and the monoclonal antisyntaxin 1 (lane 3). The two isoforms (upper arrow, 210 kDa; lower arrow, 180 kDa) of the α_{1D} subunit were pulled down only by the polyclonal antisyntaxin 1 (lane 1). The experiments were repeated two times.

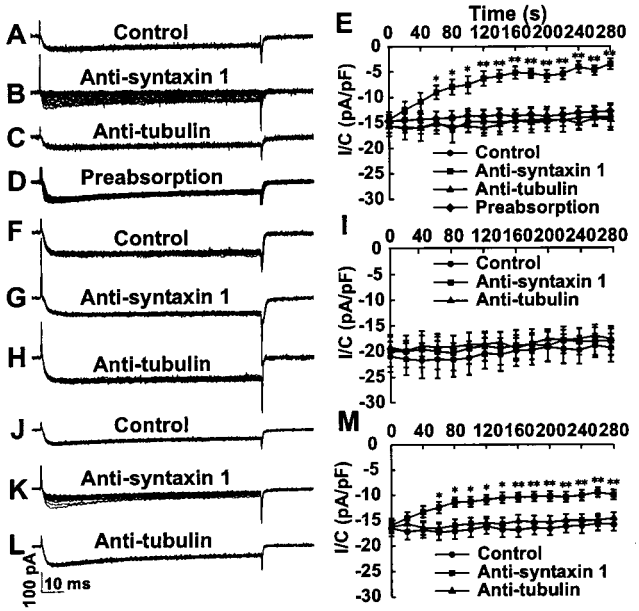

FIG. 3. Effect of antisyntaxin 1 on L type Ca^{2+} currents in mouse pancreatic β cells. (*A, C,* and *D*) Typical whole-cell patch-clamp recordings with 15 superimposed L type Ca^{2+} current traces, evoked by depolarizing voltage steps from -70 mV to 0 mV (100 ms, 0.05 Hz). Currents were similar after incubation of pancreatic β cells with extracellular solution, antitubulin (1:200), and antisyntaxin 1 (1:200) preabsorbed with GST-syntaxin 1A (240 μg/ml diluted antibody), respectively, for 1 h. (*B*) After incubation with antisyntaxin 1 (1:200), the Ca^{2+} currents decreased with the application of the depolarizing command voltage pulses. (*E*) Compiled data on changes in current amplitude showed that L type Ca^{2+} currents ran down faster in cells incubated with antisyntaxin 1 (■, $n = 10$) compared with the control cells (●, $n = 9$), cells incubated with antitubulin (▲, $n = 10$) and cells incubated with antisyntaxin 1 preabsorbed with GST-syntaxin 1A (◆, $n = 11$). The recordings were made in 10 mM Ca^{2+} at room temperature. (*F–H*) Representative whole-cell patch-clamp recordings using the same voltage step protocol, but exchanging Ca^{2+} for Ba^{2+}, showed no difference in the obtained currents after the incubation of pancreatic β cells with extracellular solution, antisyntaxin 1, and antitubulin, respectively. (*I*) Time courses of L type Ca^{2+} currents in cells incubated with antisyntaxin 1 (■, $n = 8$) were not significantly different in amplitude from those in control cells (●, $n = 8$) and cells incubated with antitubulin (▲, $n = 8$). (*J* and *L*) Typical whole-cell patch-clamp recordings with 15 superimposed L type Ca^{2+} current traces, evoked by the above-mentioned voltage-step protocol, showed similar currents after the incubation of pancreatic β cells in extracellular solution containing 10 mM Ca^{2+}/10 mM Ba^{2+} with and without antitubulin (1:200) for 1 h. (*K*) After incubation with antisyntaxin 1 (1:200) in the presence of 10 mM Ca^{2+}/10 mM Ba^{2+}, the Ca^{2+} currents decreased gradually after application of the depolarizing command voltage pulses. (*M*) Compiled data on changes in current amplitude showed that L type Ca^{2+} currents ran down faster in cells incubated with antisyntaxin 1 (■, $n = 18$) compared with control cells (●, $n = 17$) and cells incubated with antitubulin (▲, $n = 18$). The data are presented as means ± SEM. Statistical significance was evaluated by one-way ANOVA followed by least significant difference (LSD) test. *, $P < 0.05$; **, $P < 0.01$.

superimposed Ca^{2+} current traces evoked by the same voltage protocol showed similar currents after the incubation of pancreatic β cells with extracellular solution, antitubulin, and antisyntaxin 1, respectively. Compiled data show that the time courses of whole-cell L type Ca^{2+} currents in cells incubated with antisyntaxin 1 did not differ significantly from those in control cells or in cells incubated with antitubulin (Fig. 3*I*). Thus, the blocking effect of antisyntaxin 1 on Ca^{2+} channel activity disappeared after replacement of extracellular Ca^{2+} with Ba^{2+}. Furthermore, 10 mM Ca^{2+} together with 10 mM Ba^{2+} in the extracellular solution could partly restore the effect

of antisyntaxin 1 on Ca^{2+} currents. As seen in Fig. 3 *J* and *L*, the same voltage protocol as above produced similar superimposed current traces in the presence of antitubulin and under control conditions. By contrast, antisyntaxin 1 treatment promoted a significantly faster run-down of Ca^{2+} currents when recorded in 10 mM Ca^{2+} together with 10 mM Ba^{2+} (Fig. 3*K*), although this effect was smaller than that in extracellular solution containing 10 mM Ca^{2+} alone (Fig. 3*B*). Compiled data (Fig. 3*M*) show that L type Ca^{2+} currents decreased significantly faster in cells incubated with antisyntaxin 1 in comparison with control cells or cells incubated with antitubulin.

Effects of Antisyntaxin 1 and Anti-α_{1D} Subunit of the L type Ca^{2+} Channel on Exocytosis of Insulin from Pancreatic β Cells. Fig. 4 shows amperometric recordings from single cells under control conditions (Fig. 4*A*) or when pretreated with antisyntaxin 1 (1:200, Fig. 4*B*), antitubulin (1:200, Fig. 4*C*), or antisyntaxin 1 (1:200) preabsorbed with GST-syntaxin 1 (Fig. 4*D*, 240 μg/ml diluted antibody), during a short pulse of 50 mM K^+. Each amperometric spike represents the oxidation current of serotonin molecules released from individual vesicles. A pulse of 50 mM K^+ potently and rapidly induced a similar magnitude of secretion in cells preincubated with extracellular solution (64.3 $\pm$ 5.0 spikes/30 s, $n = 6$), antitubulin (61.0 $\pm$ 7.3 spikes/30 s, $n = 6$), and antisyntaxin 1 preabsorbed with GST-syntaxin 1A (43.7 $\pm$ 4.5 spikes/30 s, $n = 6$), whereas preincubation with antisyntaxin (9.8 $\pm$ 3.4 spikes/30 s, $n = 6$) dramatically decreased the number of secretory events ($P < 0.01$) (Fig. 4*E*).

Our data with an antisyntaxin 1-induced decrease in secretory response evoked by depolarization by K^+ in the intact pancreatic β cell using amperometric measurements raised the question of whether this effect resulted from a direct effect on the exocytotic machinery or whether it was partly a consequence of the decreased activity of the voltage-dependent Ca^{2+} channel. To address this question, we also tested the effect of monoclonal antisyntaxin 1 on Ca^{2+}-independent insulin secretion. In single mouse pancreatic β cells preloaded with 5-HTP, hypertonic solution (500 mOsM sucrose) was employed to trigger Ca^{2+}-independent exocytosis. Hypertonic solution-triggered exocytosis is independent of extracellular Ca^{2+} concentration, the Ca^{2+} channel blocker Cd^{2+}, and manipulation of intracellular Ca^{2+} stores (19). Fig. 5 *A* and *B* shows typical examples of the secretory response after application of 500 mOsM sucrose (as indicated by horizontal bars) to the control group (Fig. 5*A*) and to the cells (Fig. 5*B*) treated with antisyntaxin 1 (1:200). As seen from the compiled data (Fig. 5*C*) of the number of spikes during a 30-s period of hypertonic stimulation, there is no significant difference between control and antisyntaxin 1-treated groups (11.4 $\pm$ 1.8 vs. 10.9 $\pm$ 1.6, $n = 10$, $P > 0.05$). Furthermore, insulin release was assessed in electroporated pancreatic β cells challenged by 10 μM Ca^{2+} and/or 100 μM Ba^{2+}. Capacitance measurements have shown that Ba^{2+} can be used instead of Ca^{2+} to stimulate exocytosis in RINm5F insulin-secreting cells (20). The use of permeabilized cells eliminates ion fluxes through ion channels and, thus, allows analysis of direct effects on the exocytotic machinery. As shown in Fig. 6, the antisyntaxin 1 treatment (1:200) produced no significant influence on basal insulin secretion in the absence of both Ca^{2+} and Ba^{2+}, as compared with control and IgG treatment (1:200). However, insulin release from permeabilized pancreatic β cells treated with antisyntaxin 1 in the presence of 10 μM Ca^{2+} was attenuated significantly in comparison with that evoked from cells treated with IgG or preincubated in control buffer. Interestingly, Ba^{2+} (100 μM)-induced insulin release was not significantly different between cells preincubated with antisyntaxin 1, IgG, or normal intracellular buffer. The inhibitory effect of antisyntaxin on insulin release was partly restored by adding 10 μM Ca^{2+} to the solution containing 100 μM Ba^{2+}.

Whereas treatment with antisyntaxin 1 reduced the secretory response in intact cells by approximately 80%, the same treatment led to a reduction by about 40% (10 μM Ca^{2+}) and 30% (10 μM Ca^{2+} plus 100 μM Ba^{2+}) in permeabilized cells. Thus, it appears that part of the inhibitory effect on insulin

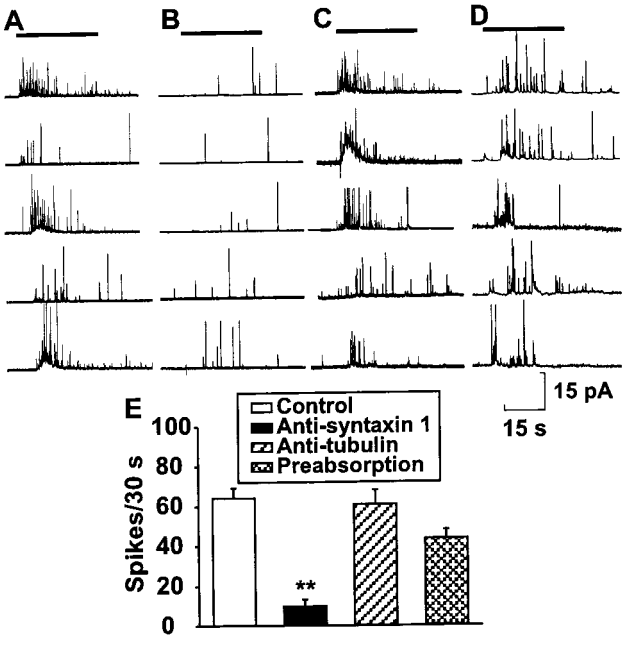

FIG. 4. Effect of monoclonal antisyntaxin 1 on exocytosis in single mouse pancreatic β cells preloaded with 5-HTP. Typical examples of the secretory response after stimulation with 50 mM K^+ (as indicated by horizontal bars) in the control group (*A*), after treatment with antisyntaxin 1 (1:200) (*B*), after treatment with antitubulin (1:200) (*C*), and after treatment with antisyntaxin 1 (1:200) preabsorbed with GST-syntaxin 1A (*D*). (*E*) Compiled data of the number of spikes during a 30-s period under each experimental condition. The data are presented as means $\pm$ SEM ($n = 6$). Statistical significance was evaluated by one-way ANOVA followed by least significant difference test. **, $P < 0.01$ vs. control, antitubulin, and antisyntaxin 1 preabsorbed with GST-syntaxin 1A.

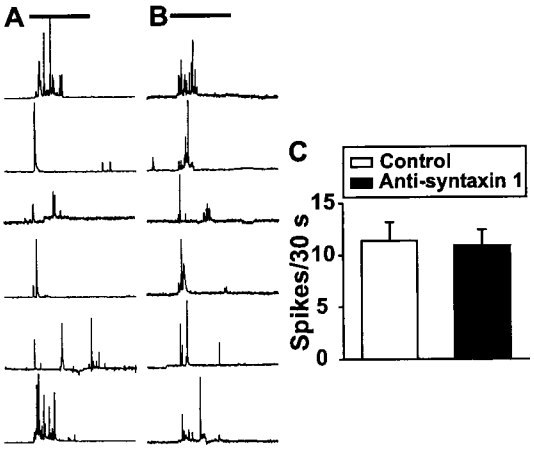

FIG. 5. Effect of monoclonal antisyntaxin 1 on exocytosis induced by application of hypertonic solution in single mouse pancreatic β cells preloaded with 5-HTP. Typical examples of the secretory response after application of 500 mOsM sucrose (as indicated by horizontal bars) in the control group (*A*) and in the cells treated with antisyntaxin 1 (1:200) (*B*). (*C*) Compiled data of the number of spikes during a 30-s period under each experimental condition. The data are presented as means $\pm$ SEM ($n = 10$). Statistical significance was evaluated by Student's *t* test. There is no significant difference between the two groups.

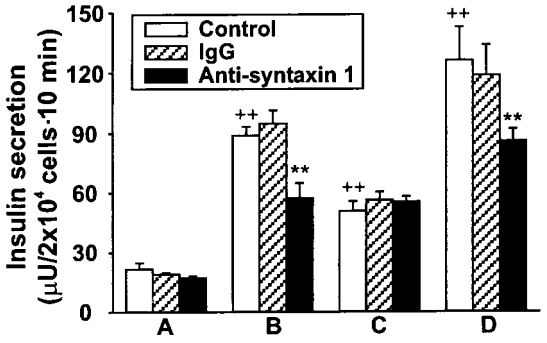

FIG. 6. Effect of mAb against syntaxin 1 on insulin release from electropermeabilized mouse pancreatic β cells. Permeabilized cells were incubated with normal intracellular buffer, monoclonal antisyntaxin 1 (1:200), and mouse IgG (1:200) in the absence of both Ca^{2+} and Ba^{2+} (*A*), in the presence of 10 μM Ca^{2+} (*B*) or 100 μM Ba^{2+} (*C*), and in the presence of 10 μM Ca^{2+} together with 100 μM Ba^{2+} (*D*). The released insulin was determined by radioimmunoassay. The data are presented as means ± SEM ($n = 6$). Statistical significance was evaluated by one-way ANOVA followed by least significant difference test. **, $P < 0.01$ vs. the absence of both Ca^{2+} and Ba^{2+}, ++, $P < 0.01$ vs. control and IgG groups in the presence of 10 μM Ca^{2+}.

secretion from intact β cells depends on reduced L type Ca^{2+} currents induced by antisyntaxin treatment.

Anti-α_{1D} was used to test whether the α_{1D} subunit of the voltage-gated Ca^{2+} channel functions as a structural base for docking/priming/fusion of insulin-containing granules with the plasma membrane. Insulin release, measured by radioimmunoassay, in permeabilized β cells incubated with anti-α_{1D} subunit (1:100) did not differ significantly from that in control cells or cells treated with IgG (1:100) (data not shown). These negative findings do not exclude that the α_{1D} subunit has a structural function in insulin exocytosis but, rather, may suggest that anti-α_{1D} does not recognize the α_{1D} subunit *in situ* and/or that the epitope on the α_{1D} subunit recognized by the antibody is not an active site in exocytosis.

DISCUSSION

We now show that syntaxin 1 and the α_{1D} subunit of the L type Ca^{2+} channel colocalize in the β cell plasma membrane by means of coexpression of the EGFP-linked α_{1D} subunit with the EBFP-linked syntaxin 1 and Western blot analysis together with subcellular fractionation. These data provide the molecular basis for a modulatory effect of syntaxin 1 on L type Ca^{2+} channel activity. Interestingly, the polyclonal antibody against the intracellular domain of syntaxin 1 efficiently coimmunoprecipitated the α_{1D} subunit from the plasma membrane fractions, whereas the mAb against the extracellular domain of syntaxin 1 did not. In this context, it is interesting to note that microinjection of the fragment 1–267 of syntaxin 1, lacking only the transmembrane domain, had no effect on the coexpressed L_C type Ca^{2+} channel, but the expressed full-length syntaxin 1 significantly modified the coexpressed L_C type Ca^{2+} channel activity in the *Xenopus* oocyte (7). The binding of the mAb against the extracellular domain of syntaxin 1 thus may mask the syntaxin-interaction site at the α_{1D} subunit and/or result in a conformational change of the interaction site of syntaxin, thereby preventing protein–protein interaction between syntaxin 1 and the α_{1D} subunit. Indeed, the interaction site of syntaxin 1 with α_{1B} and α_{1C} subunits of the Ca^{2+} channel has been shown to be close to the extracellular domain and far from the intracellular domain of syntaxin 1 (21).

In agreement with the coimmunoprecipitation data, our electrophysiological results clearly demonstrate the presence of a functional interaction between syntaxin 1 and the L type Ca^{2+} channel to maintain functional L type Ca^{2+} channel activity. Cells incubated with antisyntaxin 1 in 10 mM extracellular Ca^{2+} showed a significant decrease in L type Ca^{2+} currents. That this effect on the L type Ca^{2+} channel reflected a specific interaction between antisyntaxin 1 and syntaxin 1 was suggested from the experiments demonstrating no effect when cells were incubated in normal extracellular solution in the presence of antitubulin or antisyntaxin 1 preabsorbed with syntaxin 1. Antisyntaxin recognizes a part of the carboxyl terminus (residues 181–288) of syntaxin 1 (22, 23), which, in turn, has been demonstrated to overlap, or to be situated nearby, the site at which the syntaxin molecule interacts with the α_{1B} subunit of the N type Ca^{2+} channel in a Ca^{2+}-dependent manner (18, 21). Our results suggest that syntaxin 1 also forms a complex with the α_{1D} subunit of the L type Ca^{2+} channel and thereby prevents Ca^{2+} channel run-down. This effect is likely to be Ca^{2+}-dependent because antisyntaxin 1 failed to affect Ca^{2+} channel activity when Ca^{2+} was exchanged for Ba^{2+}. In the presence of Ba^{2+} alone, the Ca^{2+}-dependent interaction between syntaxin and the α_{1D} subunit can no longer take place and Ca^{2+}-mediated Ca^{2+} channel run-down is not activated (24, 25). Therefore, antisyntaxin 1 is without inhibitory effect on the Ba^{2+} current. The effect of antisyntaxin 1 on the Ca^{2+} channel was restored partly by the addition of Ca^{2+} to the Ba^{2+} solution. Noteworthy is that binding of antisyntaxin 1 to syntaxin 1 occurred independent of Ca^{2+} because Western blot analysis shows that antisyntaxin 1 binds to syntaxin 1 in the absence of Ca^{2+}.

The H3 region of the syntaxin 1 molecule, corresponding to amino acids 191–285, has been shown to be important in the interactions of syntaxin with other proteins that participate in the secretory process (2). This region was demonstrated to be involved in Ca^{2+}-induced secretion in permeabilized β cells (2). In the present study we investigated the effects of antisyntaxin 1 on both intact and permeabilized mouse β cells, showing a more pronounced inhibitory effect in intact cells. Thus, whereas insulin release from permeabilized cells treated with antisyntaxin was decreased by approximately 40%, challenged by 10 μM Ca^{2+} alone, antisyntaxin 1 reduced the secretory response by about 80% in intact cells. In accordance with Ca^{2+} channel data, Ba^{2+}-induced exocytosis was not inhibited by antisyntaxin 1. Furthermore, there is no significant difference in Ca^{2+}-independent insulin release, evoked by hypertonic stimulation, between antisyntaxin-treated and control groups. The antisyntaxin 1 treatment did not influence basal insulin secretion from permeabilized mouse β cells in the absence of both Ca^{2+} and Ba^{2+}. It, therefore, is reasonable to assume that the more pronounced inhibitory effect in intact cells was due to the decreased activity of the L type Ca^{2+} channel by treatment with antisyntaxin 1. In agreement with the patch-clamp data, addition of Ca^{2+} to the Ba^{2+} buffer regained the inhibitory effect of antisyntaxin on insulin release from permeabilized cells. The coexpressed α_{1C} subunit and syntaxin 1 have been demonstrated to interact with each other in the *Xenopus* oocyte (7, 8). The *in vitro* binding of a synthetic peptide fragment ($L_{C753-893}$) of the α_{1C} subunit to GST-syntaxin 1 also has been documented (8). Moreover, it has been shown that the synthetic peptide of the α_{1C} subunit interfered with the interaction between the native L_C type Ca^{2+} channel and the exocytotic machinery in the pancreatic β cell (8). However, it is worth noting that there is a much higher level of mRNA encoding the α_{1D} subunit than the α_{1C} subunit in the pancreatic β cell (9, 10). Our preliminary data indicate a stronger α_{1D} subunit signal than α_{1C} subunit signal in the plasma membrane of the pancreatic β cell (data not shown). Therefore, it is likely that the α_{1D} subunit is the major α_1 subunit interacting with syntaxin in the pancreatic β cell.

Interestingly, insulin release from control permeabilized cells evoked by 10 μM Ca^{2+} plus 100 μM Ba^{2+} was approximately equal to the sum of insulin release evoked by either divalent cation alone. This suggests that Ba^{2+} has a different

binding site than Ca^{2+} in the activation of the exocytotic process. It indeed has been demonstrated that Ba^{2+} triggers exocytosis in permeabilized chromaffin cells by an effect on the exocytotic machinery that is different from that induced by Ca^{2+} (26). Furthermore, depletion of intracellular Ca^{2+} stores by thapsigargin fully blocks Ca^{2+}-triggered exocytosis, but only slightly affects Ba^{2+}-induced insulin secretion in this cell line (20).

We have shown that syntaxin 1 interacts with the α_{1D} subunit of the voltage-gated L type Ca^{2+} channel and that binding of antisyntaxin 1 to syntaxin 1 interferes with the regulation of both the voltage-gated L type Ca^{2+} channel and the exocytotic machinery in insulin-secreting pancreatic β cells. This may reflect an interference with the assembly of the α_{1D} subunit, syntaxin 1, and synaptic vesicle proteins, which are located in the insulin-containing granule, into a functioning core complex. This suggests that the L_D type Ca^{2+} channel has a similar structure–function relationship with the exocytotic machinery as has been described previously for the neuronal N type Ca^{2+} channel (27). Thus, the ability of syntaxin to modulate overall neuroendocrine secretion seems to have a general explanation at the molecular level.

We are grateful to Dr. William A. Catterall for providing GST-syntaxin 1. This work was supported by grants from the Swedish Medical Research Council (03X-09891, 03X-09890, 03XS-12708, 72X-12549, and 19X-00034), the Swedish Diabetes Association, the Nordic Insulin Foundation Committee, Funds of Karolinska Institutet, Berth von Kantzows Foundation, Juvenile Diabetes Foundation International, the Swedish Society for Medical Research, and the Novo Nordisk Foundation.

1. Martin, F., Moya, F., Gutierrez, L. M., Reig, J. A. & Soria, B. (1995) *Diabetologia* **38,** 860–863.
2. Martin, F., Salinas, E., Vazquez, J., Soria, B. & Reig, J. A. (1996) *Biochem. J.* **320,** 201–205.
3. Nagamatsu, S., Fujiwara, T., Nakamichi, Y., Watanabe, T., Katahira, H., Sawa, H. & Akagawa, K. (1996) *J. Biol. Chem.* **271,** 1160–1165.
4. el Far, O., Charvin, N., Leveque, C., Martin-Moutot, N., Takahashi, M. & Seagar, M. J. (1995) *FEBS Lett.* **361,** 101–105.
5. Martin-Moutot, N., Charvin, N., Leveque, C., Sato, K., Nishiki, T., Kozaki, S., Takahashi, M. & Seagar, M. (1996) *J. Biol. Chem.* **271,** 6567–6570.
6. Bezprozvanny, I., Scheller, R. H. & Tsien, R. W. (1995) *Nature (London)* **378,** 623–626.
7. Wiser, O., Bennett, M. K. & Atlas, D. (1996) *EMBO J.* **15,** 4100–4110.
8. Wiser, O., Trus, M., Hernández, A., Renström, E., Barg, S., Rorsman, P. & Atlas, D. (1999) *Proc. Natl. Acad. Sci. USA* **96,** 248–253.
9. Iwashima, Y., Pugh, W., Depaoli, A. M., Takeda, J., Seino, S., Bell, G. I. & Polonsky, K. S. (1993) *Diabetes* **42,** 948–955.
10. Seino, S., Chen, L., Seino, M., Blondel, O., Takeda, J., Johnson, J. H. & Bell, G. I. (1992) *Proc. Natl. Acad. Sci. USA* **89,** 584–588.
11. Hellman, B. (1965) *Ann. N. Y. Acad. Sci.* **131,** 541–558.
12. Chibalin, A. V., Katz, A. I., Berggren, P.-O. & Bertorello, A. M. (1997) *Am. J. Physiol.* **273,** C1458–C1465.
13. Brown, H., Larsson, O., Bränström, R., Yang, S.-N., Leibiger, B., Leibiger, I., Fried, G., Moede, T., Deeney, J. T., Brown, G. R., *et al.* (1998) *EMBO J.* **17,** 5048–5058.
14. Aspinwall, C. A., Brooks, S. A., Kennedy, R. T. & Lakey, J. R. (1997) *J. Biol. Chem.* **272,** 31308–31314.
15. Efanov, A. M., Zaitsev, S. V. & Berggren, P.-O. (1997) *Proc. Natl. Acad. Sci. USA* **94,** 4435–4439.
16. Hundal, H. S., Maxwell, D. L., Ahmed, A., Darakhshan, F., Mitsumoto, Y. & Klip, A. (1994) *Mol. Membr. Biol.* **11,** 255–262.
17. Hell, J. W., Westenbroek, R. E., Warner, C., Ahlijanian, M. K., Prystay, W., Gilbert, M. M., Snutch, T. P. & Catterall, W. A. (1993) *J. Cell Biol.* **123,** 949–962.
18. Sheng, Z. H., Rettig, J., Cook, T. & Catterall, W. A. (1996) *Nature (London)* **379,** 451–454.
19. Rosenmund, C. & Stevens, C. F. (1996) *Neuron* **16,** 1197–1207.
20. Richmond, J. E., Codignola, A., Cooke, I. M. & Sher, E. (1996) *Pflügers Arch.* **432,** 258–269.
21. Sheng, Z. H., Rettig, J., Takahashi, M. & Catterall, W. A. (1994) *Neuron* **13,** 1303–1313.
22. Bennett, M. K., Garcia-Arraras, J. E., Elferink, L. A., Peterson, K., Fleming, A. M., Hazuka, C. D. & Scheller, R. H. (1993) *Cell* **74,** 863–873.
23. Inoue, A., Obata, K. & Akagawa, K. (1992) *J. Biol. Chem.* **267,** 10613–10619.
24. Hofer, G. F., Hohenthanner, K., Baumgartner, W., Groschner, K., Klugbauer, N., Hofmann, F. & Romanin, C. (1997) *Biophys. J.* **73,** 1857–1865.
25. Schuhmann, K., Romanin, C., Baumgartner, W. & Groschner, K. (1997) *J. Gen. Physiol.* **110,** 503–513.
26. Heldman, E., Levine, M., Raveh, L. & Pollard, H. B. (1989) *J. Biol. Chem.* **264,** 7914–7920.
27. Mochida, S., Sheng, Z. H., Baker, C., Kobayashi, H. & Catterall, W. A. (1996) *Neuron* **17,** 781–788.